Dark energy at early times, the Hubble parameter, and the string axiverse

Tanvi Karwal and Marc Kamionkowski

Phys. Rev. D **94**, 103523 — Published 28 November 2016

DOI: 10.1103/PhysRevD.94.103523

Early dark energy, the Hubble-parameter tension, and the string axiverse

Tanvi Karwal and Marc Kamionkowski
Department of Physics and Astronomy, Johns Hopkins University, 3400 N. Charles St., Baltimore, MD 21218

Precise measurements of the cosmic microwave background (CMB) power spectrum are in excellent agreement with the predictions of the standard ΛCDM cosmological model. However, there is some tension between the value of the Hubble parameter H_0 inferred from the CMB and that inferred from observations of the Universe at lower redshifts, and the unusually small value of the dark-energy density is a puzzling ingredient of the model. In this paper, we explore a scenario with a new exotic energy density that behaves like a cosmological constant at early times and then decays quickly at some critical redshift z_c. An exotic energy density like this is motivated by some string-axiverse-inspired scenarios for dark energy. By increasing the expansion rate at early times, the very precisely determined angular scale of the sound horizon at decoupling can be preserved with a larger Hubble constant. We find, however, that the Planck temperature power spectrum tightly constrains the magnitude of the early dark-energy density and thus any shift in the Hubble constant obtained from the CMB. If the reionization optical depth is required to be smaller than the Planck 2016 2σ upper bound $\tau \lesssim 0.0774$, then early dark energy allows a Hubble-parameter shift of at most 1.6 km s^{-1} Mpc^{-1} (at $z_c \simeq 1585$), too small to fully alleviate the Hubble-parameter tension. Only if τ is increased by more than 5σ can the CMB Hubble parameter be brought into agreement with that from local measurements. In the process, we derive strong constraints to the contribution of early dark energy at the time of recombination—it can never exceed $\sim 2\%$ of the radiation/matter density for $10 \lesssim z_c \lesssim 10^5$.

I. INTRODUCTION

Current measurements of temperature and polarization power spectra of the cosmic microwave background (CMB) are in excellent agreement with the standard ΛCDM cosmological model [1]. Still, there is some tension between the value $H_0 = 66.93 \pm 0.62$ km s^{-1} Mpc^{-1} of the Hubble parameter obtained from the CMB [2] and those obtained from local measurements, $H_0 = 73.24 \pm 1.74$ km s^{-1} Mpc^{-1} (3.4σ tension) as inferred from supernovae and more [3], and $H_0 = 72.8 \pm 2.4$ km s^{-1} Mpc^{-1} as measured by H0LiCOW [4]. There is also unease among some theorists about the incredibly small value, relative to the Planck density, of the dark-energy density required to account for the observations [5]. There are an almost endless number of explanations for dark energy, but this work will be inspired by a recently proposed string-axiverse [6–9] scenario for dark energy [10].

The purpose of this paper is to investigate whether the Hubble-parameter tension might be explained by the presence of an exotic dark-energy density in the early Universe of the type that might arise in some of these axiverse scenarios. In this framework, dark energy is due to an axion-like field that is active today [9, 10]. However, there can be a large number of similar light fields that can be dynamically important at some point in the earlier history of the Universe and then decay away in influence.

Here we surmise that one of these axion-like fields becomes dynamical around the time of recombination. More precisely, it behaves, as we will delineate more clearly below, like a cosmological constant at early times. However, at some critical redshift z_c, which is taken to be on order the redshift of recombination, the energy density then decays more rapidly than that of radiation. The cosmological-constant–like behavior at early times increases the pre-recombination expansion rate and thus reduces the sound horizon at recombination. The resulting reduction in the angle subtended by the CMB acoustic peaks can then be compensated by an increase in the Hubble constant.

Although such an exotic early dark energy is capable of increasing the value of the Hubble parameter today, we find that a value of τ greater than its Planck-2016 2σ upper bound is required to fully resolve the Hubble tension. We also find that the exotic energy (EE) is constrained to contribute at most $\sim 2\%$ of the total energy density of a ΛCDM universe around the time of recombination, and may only contribute $\gtrsim 5\%$ if it decays earlier than a redshift of $\sim 10^5$.

The idea of an additional early-Universe contribution to the energy density has been considered before [11–13]. Although similar in spirit, those models differ from what we consider here. The conclusion reached in our work that EE contributes no more than $\sim 2\%$ of the critical density around the time of recombination is consistent with the conclusions of earlier papers on other early-dark-energy models in which upper limits of $\sim 4-5\%$ were inferred. The increased early-Universe expansion rate considered here also resembles in spirit the explanation suggested in Refs. [3, 13, 14] for the Hubble-parameter tension in terms of an increased number of relativistic degrees of freedom.

This paper is organized as follows. In Section II, we describe the exotic energy model, its evolution and its effect on the TT spectrum. In Section III, we describe the Fisher-matrix analysis we employ to constrain the model (Section III A) and the data we use for this analysis (Sec-

tion III B). In Section IV we obtain constraints on the EE and determine how it changes the Hubble parameter. We do so for the optical depth at reionisation τ fixed at its current best-fit (Section IV A), 2σ (Section IV B) and 5σ (Section IV C) values. We conclude in Section V.

II. MODEL

The form of the exotic energy (EE) we consider is motivated by the axion-like fields discussed in Ref. [10]. There it was argued that an axion-like field driving accelerated expansion today might be one of ~ 100 such fields in the string axiverse, each of which has some small chance to drive accelerated expansion at some point in the history of the Universe. The scenario suggests that there may be other axion-like fields that may have behaved earlier in the history of the Universe like a cosmological constant but then decayed away in influence.

Here we will use a phenomenological model inspired by Ref. [10]. The energy density $\rho_{\rm ee}$ of the EE takes the form,

$$\frac{\rho_{\rm ee}(a)}{\rho_c} = \frac{\Omega_{\rm ee}(1+a_c^6)}{a^6+a_c^6}, \tag{1}$$

where ρ_c is the critical density today, $\Omega_{\rm ee}$ is the fractional energy density of the EE today and $a_c = 1/(1+z_c)$ is the critical value of the scale factor at which the EE shifts from early-time behavior to late-time behavior.

The pressure the EE exerts is

$$p_{\rm ee}(a) = \rho_{\rm ee}\frac{a^6-a_c^6}{a^6+a_c^6}. \tag{2}$$

It can be seen that at redshifts $z \gg z_c$, we have $a^6 \ll a_c^6$ and therefore $p_{ee} \simeq -\rho_{ee}$. That is, the EE behaves like a cosmological constant at early times, similar to a slowly rolling axion field. On the other hand, at redshifts $z \ll z_c$, $a^6 \gg a_c^6$ and $p_{ee} \simeq \rho_{ee}$, emulating a free scalar field, with the hardest possible equation of state allowed by causality.

Fig. 1 shows how the energy density of the EE evolves over cosmic history. Matter, radiation and the cosmological constant are also shown for comparison. Changing $\Omega_{\rm ee}$ shifts the curve of the EE up or down. Changing z_c changes the redshift at which the EE switches from behaving like a cosmological constant to decaying away faster than radiation.

We assume that the EE only changes the homogeneous background evolution of the universe. We do not have a physical model of how perturbations change as a result of adding this phenomenological model to ΛCDM. In this paper, we simply add the energy density and pressure of the EE to the Friedmann equation in the background sector of the public code Cosmic Linear Anisotropy Solving System (CLASS) [15]. We note that inclusion of scalar-field perturbations can, in some cases, considerably alter the perturbation spectrum [16]. We will address the effects of perturbations in realistic, physical models for EE in subsequent work.

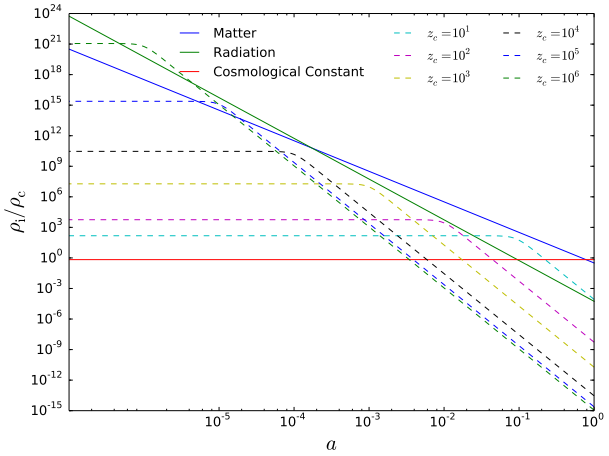

FIG. 1. Shown here are the evolutions of the energy densities of exotic energy (EE; dashed lines) for several critical redshifts z_c, matter (solid blue), radiation (solid green), and the cosmological constant (solid red). For each z_c we choose the exotic-energy density $\Omega_{\rm ee}$ to be the 3σ upper limit we derive from the Planck temperature power spectrum assuming the reionization optical depth τ is fixed to the current Planck best-fit value. The energy densities are all shown, relative to the critical density ρ_c today, as a function of the scale factor a.

On adding such an EE with non-zero $\Omega_{\rm ee}$ to ΛCDM, the predicted TT angular power spectrum will shift. It can be shifted back to better fit the data by shifting the other parameters of the ΛCDM model. We show how EEs of various z_c and $\Omega_{\rm ee}$ shift the TT spectrum in Fig. 2.

For our analysis, we choose the critical redshift range $10 \leq z_c \leq 10^6$. We found that critical redshifts smaller than approximately 500 shift the angular size θ_* of the sound horizon at recombination to larger values for $\Omega_{\rm ee} > 0$. If θ_* were increased in this way, then the current expansion rate H_0 would have to be decreased to shift θ_* back to its measured value. EEs with $z_c \lesssim 500$ therefore move the Hubble parameter further away from its local value, exacerbating the discrepancy between the Planck and local values. We include some such critical redshifts in our analysis, limiting the z_c range to 10 on the lower end.

On the higher end, we limit our analysis to $z_c \leq 10^6$, as EEs with higher critical redshifts have little effect on CMB power spectra.

III. METHOD

Our aim here is to determine the largest value of the fractional exotic energy density $\Omega_{\rm ee}$ consistent with Planck measurements of the temperature power spec-

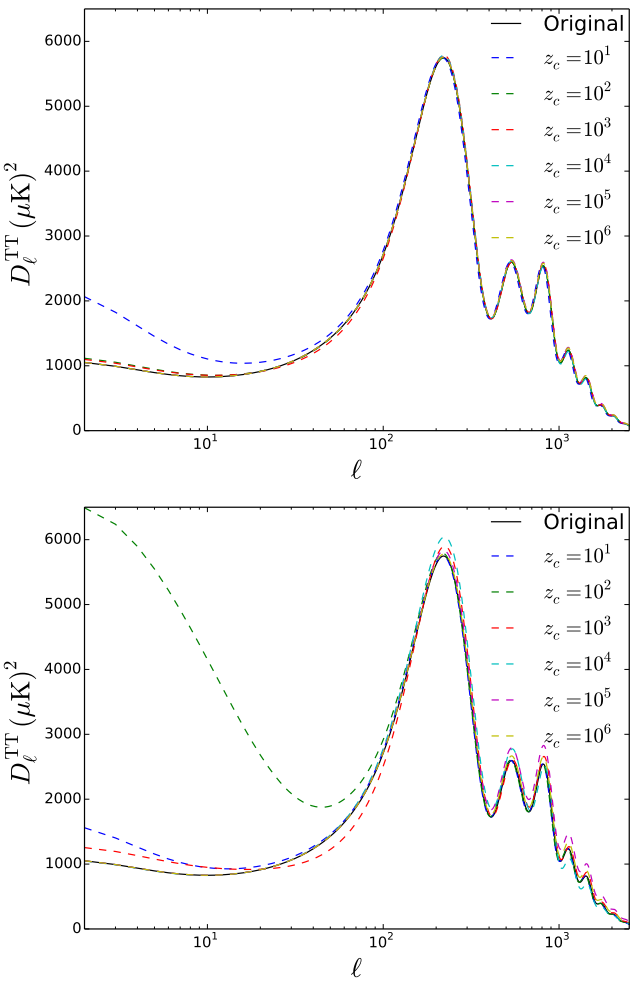

FIG. 2. The shifts caused in the TT power spectrum due to the addition of EE are shown for various z_c. Here, the value of the reionization optical is fixed to the current Planck best-fit value $\tau = 0.0596$. The other cosmological parameters are fixed at the values, shown in Table I, that provide the best fit to the TT power spectrum. Clearly the critical redshift of the EE is important in determining how the EE shifts the TT spectrum. In the upper figure, the value of $\Omega_{\rm ee}$ chosen for each z_c is the 3σ upper limit of its best fit. In the lower figure, $\Omega_{\rm ee}$ is chosen such that it moves θ_* by 1%. $\Omega_{\rm ee}$ is approximately two orders of magnitude greater for the lower plot.

trum[1], after marginalizing over the other cosmological parameters that are fit to the data. (While doing so, we also investigate whether a nonzero $\Omega_{\rm ee}$ is preferred by the data, but find a null result.) Given the speculative nature of the model, here we do a rough initial analysis, following that outlined in Refs. [17–20], in which the log-likelihood is approximated by a quadratic dependence on the parameters. The loss of precision of this approach, relative to the full Monte Carlo analysis, is made up for by clarity and simplicity. The upper bounds we derive, though, should be understood as approximations rather than precise results.

Given the complexities involved in the current Planck polarization data, we work here with only the temperature power spectrum. Since the primary impact of the polarization data (especially that at low multipole moments ℓ) is to fix the reionization optical depth τ [21], we remove τ from our Fisher analysis and instead fix it to different values that fall within (and, for illustration, also outside) the current Planck error limits. As we will see, the best-fit cosmological parameters we infer from the temperature power spectrum are in rough agreement (within 2σ) of those reported by the complete Planck analysis (including polarization). We believe, therefore, that the cosmological-parameter shifts we infer below from the introduction of exotic energy reflect reasonably well those that would be obtained from a complete analysis.

A. Fisher Matrices

In order to constrain $\Omega_{\rm ee}$ for various z_c's, we do a Fisher-matrix analysis using the Planck TT angular power spectrum $D_\ell^{\rm TT,obs}$ in a manner similar to that outlined in Ref. [17–20]. For the analysis, we vary $H_0 = 100h$ km s^{-1} Mpc^{-1}, the fractional density $\omega_{\rm b} = \Omega_{\rm b}h^2$ of baryons today, the fractional density $\omega_{\rm c} = \Omega_{\rm c}h^2$ of cold dark matter today, the amplitude $\ln(10^{10}A_{\rm s})$ of the primordial power spectrum, and the scalar spectral index $n_{\rm s}$. We refer henceforth to these 5 parameters in our Fisher analysis as the "cosmological parameter" and then introduce the current exotic-energy density $\Omega_{\rm ee}$, for a given z_c, as a sixth parameter in the Fisher analysis.

We parametrize the residues $R(\ell)$ of the observed and best-fit spectra as

$$\begin{aligned} R(\ell) &= D_\ell^{\rm TT,obs} - D_\ell^{\rm TT,best-fit} \\ &= \sum_{i=1}^{N_p} \delta A_i g_i^{\rm TT}(\ell). \end{aligned} \tag{3}$$

Here N_p is the total number of parameters A_i, and

$$g_i(\ell) = \frac{\partial D_\ell}{\partial A_i}. \tag{4}$$

where we have dropped the spectrum identifier TT. The partial derivatives $g_i(\ell)$ of the spectrum with respect to the cosmological parameters were determined by shifting the parameters by 1% about their best-fit values and running the CLASS code to create the TT power spectrum for each shift. Therefore, $\Delta A_i = 0.01A_i$ and the

[1] Observations obtained with Planck (http://www.esa.int/Planck), an ESA science mission with instruments and contributions directly funded by ESA Member States, NASA, and Canada.

derivatives become:

$$g_i(\ell) = \frac{D_\ell(A_i + \Delta A_i) - D_\ell(A_i - \Delta A_i)}{2\Delta A_i}. \quad (5)$$

The choice of changing all parameters by 1% is only somewhat arbitrary. We assume that this change is small enough that we are still in the linear regime, which validates the Fisher analysis and use of finite differences to numerically differentiate. Moreover, we assume a 1% shift is large enough to ensure that the partial derivatives do not suffer significant numerical errors. These partial derivatives are shown in Fig. 3.

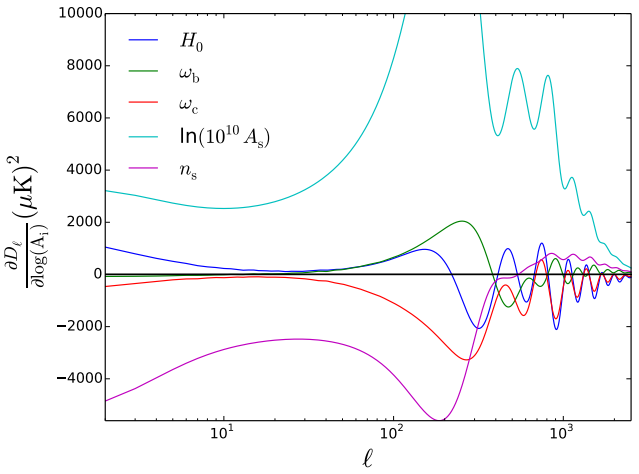

FIG. 3. Shown here are the partial derivatives of the TT spectrum with respect to the cosmological parameters, H_0 (dark blue), ω_b (green), ω_c (red), $\ln(10^{10} A_s)$ (light blue) and n_s (pink). These were derived at the best-fit values obtained by setting $\tau = \tau_{Pl}$, shown in Table I.

For the EE, the partials were determined as

$$g_{\Omega_{ee}}(\ell) = \frac{D_\ell(\Delta\Omega_{ee}) - D_\ell(\Omega_{ee} = 0)}{\Delta\Omega_{ee}}, \quad (6)$$

where $\Delta\Omega_{ee}$ is the value of Ω_{ee} that moved the angular size θ_* of the sound horizon at the redshift of the CMB by 1%. This value was found by recursively running CLASS for each z_c until a $\Delta\Omega_{ee}$ was found that moved θ_* by 1% in either direction. The partial derivatives of $D_\ell^{best-fit}$ with respect to Ω_{ee} for various z_c's are shown in Fig. 4.

The Fisher matrix F_{ij} is then given by

$$F_{ij} = \langle g_i, g_j \rangle, \quad (7)$$

where $\langle , \rangle$ denotes the inner product

$$\langle g_i, g_j \rangle \equiv \sum_l \frac{g_i(\ell) g_j(\ell)}{(\sigma_{D_\ell})^2}, \quad (8)$$

and σ_{D_ℓ} is the error on D_ℓ^{obs}. Hence, the analysis is limited by the error on the observed D_ℓ's.

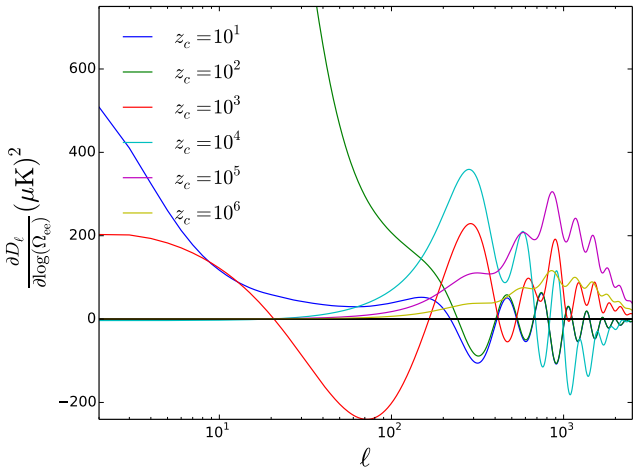

FIG. 4. The partial derivatives of the TT spectrum with respect to Ω_{ee} are shown here for various values of z_c.

The inverse Fisher matrix is then [22]

$$(F^{-1})_{ij} = r_{ij}\sigma_i\sigma_j, \quad (9)$$

where r_{ij} is the correlation coefficient between the parameters A_i and A_j, and σ_i and σ_j are their respective errors.

B. Planck Data

In their 2016 paper, Planck reports best-fit values for the TT + TE + EE + SIMLow (SimLow is based on low ℓ EE data) spectra combined [2]. We begin by using these values for the cosmological parameters and for τ; we label these as Planck-16. However, as we only use the Planck TT power spectrum for our analysis, the best-fit values for just the TT spectrum will be shifted from Planck-16 by some small amount. Therefore, we first do a Fisher analysis using just the TT spectrum and the cosmological parameters in order to find this new best fit.

The minimum-variance unbiased estimators are determined as

$$\delta A_i = \sum_j (F^{-1})_{ij} \langle R(\ell), g_j(\ell) \rangle, \quad (10)$$

where δA_i quantifies the shift, relative to Planck-16, in the parameter A_i that will fit just the TT data better. We then check that the shifts in the parameters are all small compared with their 1σ errors and furthermore that the shift in

$$\chi^2 = \sum_\ell \frac{R^2(\ell)}{(\sigma_{D_\ell})^2} = \langle R(\ell), R(\ell) \rangle \quad (11)$$

is insignificant. We thus check that

$$\sigma_i \frac{\partial \chi^2}{\partial A_i} = -2\sigma_i \langle R(\ell), g_i(\ell) \rangle \ll 1. \tag{12}$$

Doing so, we begin our investigation of the effects of exotic energy with a baseline ΛCDM model that provides the best fit to the TT data that we use and that is consistent, within errors, with the best-fit CMB values obtained from the full Planck-16 analysis. The values adopted for the cosmological parameters + τ for our subsequent analysis are shown in Table I.

As errors on higher D_ℓ's are correlated [23], we use binned data for $\ell \geq 30$. The bin size is 30 for all but the last bin which spans $2490 \leq \ell \leq 2508$. The correlation between errors on D_ℓ's from different bins is then diminished. In all, we use $2 \leq \ell \leq 2508$ for the analysis.

IV. CONSTRAINTS ON THE EE

Adding the EE will shift all parameters by some amount, which can be expressed in terms of χ^2 and the errors on the parameters as

$$\delta A_i = -\frac{1}{2} \sum_j r_{ij} \sigma_i \sigma_j \frac{\partial \chi^2}{\partial A_j}. \tag{13}$$

The quantity $\sigma_j (\partial \chi^2 / \partial A_j)$ is small at the best-fit value for the cosmological parameters and the correlation coefficients are such that $|r_{ij}| \leq 1$. This makes the shift in any parameter δA_i due to any of the cosmological parameters much smaller than the error σ_i on A_i. Therefore, all significant shifts are due to the EE,

$$\delta A_i \simeq -\frac{1}{2} (F^{-1})_{i,\Omega_{\rm ee}} \frac{\partial \chi^2}{\partial \Omega_{\rm ee}}. \tag{14}$$

For the EE, this shift looks like

$$\delta \Omega_{\rm ee} \simeq -\frac{1}{2} (F^{-1})_{\Omega_{\rm ee},\Omega_{\rm ee}} \frac{\partial \chi^2}{\partial \Omega_{\rm ee}}. \tag{15}$$

Therefore, the shift in parameter A_i induced by a change $\Delta\Omega_{\rm ee}$ from its baseline value $\Omega_{\rm ee} = 0$ is

$$\delta A_i(z_c) \simeq \frac{(F^{-1})_{i,\Omega_{\rm ee}}}{(F^{-1})_{\Omega_{\rm ee},\Omega_{\rm ee}}} \delta \Omega_{\rm ee}, \tag{16}$$

where δA_i's are now a function of the critical redshift z_c.

Below we do the following for several values of τ: (1) We first determine the values of the five other cosmological parameters that provide the best fit to the TT data we use; (2) we then add $\Omega_{\rm ee}$ as a sixth parameter to the Fisher analysis and determine (a) the best-fit value of $\Omega_{\rm ee}$; (b) the 1σ error to $\Omega_{\rm ee}$; and (c) the shifts induced by $\Omega_{\rm ee}$ to the cosmological parameters and record specifically the shift in H_0. We provide results as a function of $10 \lesssim z_c \lesssim 10^6$. (3) We look in each case to see whether the introduction of $\Omega_{\rm ee}$ improves the fit to the TT data by a statistically significant amount. In no case do we find evidence that the TT data prefers a nonzero value of $\Omega_{\rm ee}$ and thus derive in each case only upper limits to $\Omega_{\rm ee}$.

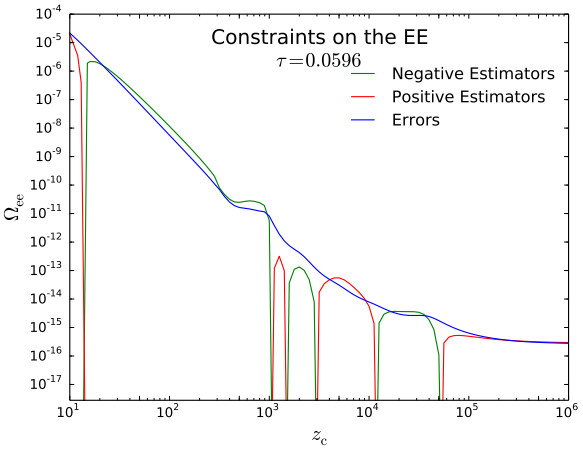

FIG. 5. The best-fit values and errors on $\Omega_{\rm ee}$ are shown here. The optical depth τ was fixed at the best-fit Planck-16 value to obtain these constrains.

A. Fixing $\tau = \tau_{\rm Pl}$

We begin by considering the current Planck central value $\tau = 0.0596$. The constraints to $\Omega_{\rm ee}$ are then shown in Fig. 5 as a function of the critical redshift z_c. Also shown there is the 1σ error to $\Omega_{\rm ee}$. The best-fit value of $\Omega_{\rm ee}$ is (unphysically) negative for some z_c, but for no value of z_c does the preferred value depart from the null result by a statistically-significant amount. This remains true for all our constraints on $\Omega_{\rm ee}$ for various values of τ.

For $\tau = 0.0596$, the largest allowable EE-induced increase in the best-fit value of the Hubble parameter is 0.22 km s^{-1} Mpc^{-1}, at a critical redshift $z_c \simeq 10000$. This is a small fraction of the Planck 1σ error (roughly 0.6 km s^{-1} Mpc^{-1}) to H_0, so does not do much in the way of relieving the CMB/local-measurement tension. The introduction of $\Omega_{\rm ee}$ to the Fisher analysis increases the error to H_0, to roughly 1.2 km s^{-1} Mpc^{-1}, and so may go some way toward alleviating the tension.

B. Fixing $\tau = \tau_{\rm Pl} + 2\sigma_{\tau,\rm Pl}$

Next we fix τ at its Planck-16 2σ upper limit. The TT spectrum prefers a larger value of τ [1]. Therefore, the reduced χ^2 is slightly smaller in this case, and smaller still when we fix τ at its 5σ Planck-16 value, as seen from Table I.

The constraints on $\Omega_{\rm ee}$ are shown in Fig. 7. We find that the errors on $\Omega_{\rm ee}$ are essentially the same between

	Planck-16	$\tau = \tau_{\rm Pl}$	$\tau = \tau_{\rm Pl} + 2\sigma_{\tau,{\rm Pl}}$	$\tau = \tau_{\rm Pl} + 5\sigma_{\tau,{\rm Pl}}$
$100h$	66.93 ± 0.62	67.99749	68.28782	68.77709
$\omega_{\rm b}$	0.02218 ± 0.00015	0.02240	0.02244	0.02251
$\omega_{\rm c}$	0.1205 ± 0.0014	0.11970	0.11906	0.11799
τ	0.0596 ± 0.0089	0.0596	0.0774	0.1041
$ln10^{10}A_{\rm s}$	3.056 ± 0.018	3.05576	3.08972	3.14024
$n_{\rm s}$	0.9619 ± 0.0045	0.96453	0.96599	0.96862
$\chi^2_{\rm red}$	0.9271	0.7652	0.7471	0.7322

TABLE I. The values of the cosmological parameters and reionization optical depth τ used as the best-fit values with no exotic energy (EE) are shown alongside the Planck values. We also show the reduced χ^2 for the TT power spectrum for these values.

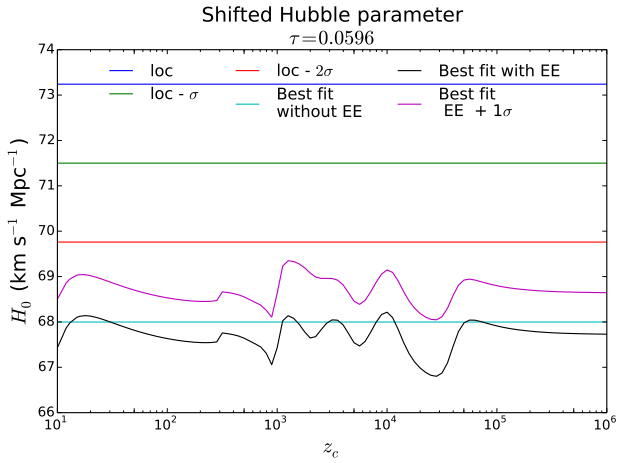

FIG. 6. Shown here are the best-fit values of the Hubble parameter H_0 and its 1σ upper limit obtained by including EEs in the fit to the Planck temperature power spectrum. We also show the central value obtained from local measurements in [3] as well as the values that are 1σ and 2σ lower than the best fit.

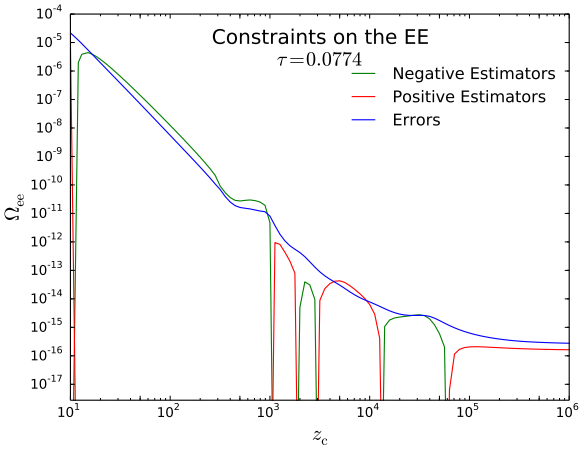

FIG. 7. The best-fit values and errors on $\Omega_{\rm ee}$ are shown for various critical redshifts of the EE. We fix τ at $\tau_{\rm Pl} + 2\sigma_{\tau,{\rm Pl}}$.

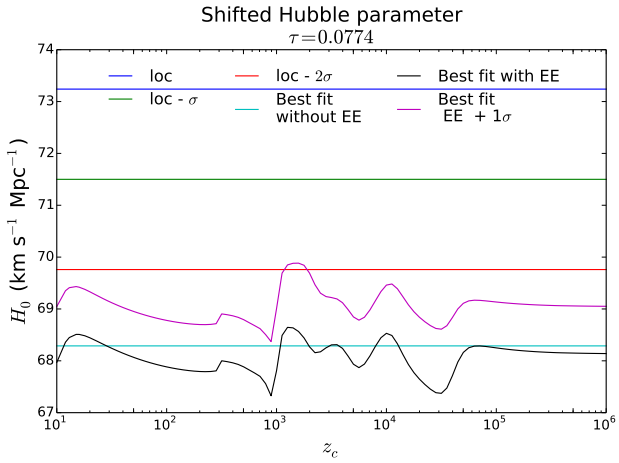

FIG. 8. The best-fit and best-fit + 1σ values for H_0 (in km s^{-1} Mpc^{-1}) are shown along with its local measurement at various σ.

our analyses at various values of τ. The blue line in Fig. 7 hence offers a visual reference to comparing constrains on $\Omega_{\rm ee}$ for various τ.

The change brought about in the Hubble parameter for $\tau = 0.0774$ is shown in Fig. 8. The best-fit value of H_0 increases at most by 0.36 km s^{-1} Mpc^{-1} ($z_c = 1259$), its 1σ value increasing at most by 1.6 km s^{-1} Mpc^{-1} ($z_c = 1585$). The total increase in the Hubble parameter for $\tau = 0.0774$ is twofold. Firstly, the EE is capable of inducing a greater positive shift in H_0 as compared to $\tau = \tau_{\rm Pl}$. Secondly, for higher τ, a larger best-fit value of H_0 without any EE is preferred, as can be seen from Table 1. Consequently, although the Hubble tension is not resolved, H_0 is pushed closer to its local measurement.

C. Fixing $\tau = \tau_{\rm Pl} + 5\sigma_{\tau,{\rm Pl}}$

The results from fixing τ at its Planck-16 and 2σ values hint that perhaps a higher value of τ will allow the EE to fully resolve the Hubble tension. Therefore, in this Section we explore what happens if τ for some reason departs by 5σ from its best-fit value. The best-fit values adopted in this section are shown in Table I.

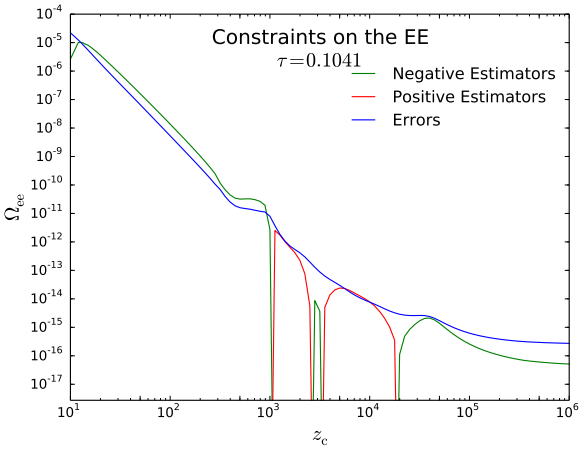

FIG. 9. The best-fit values and errors on $\Omega_{\rm ee}$ for various z_c are shown for τ fixed at $\tau_{\rm Pl} + 5\sigma_{\tau,{\rm Pl}}$.

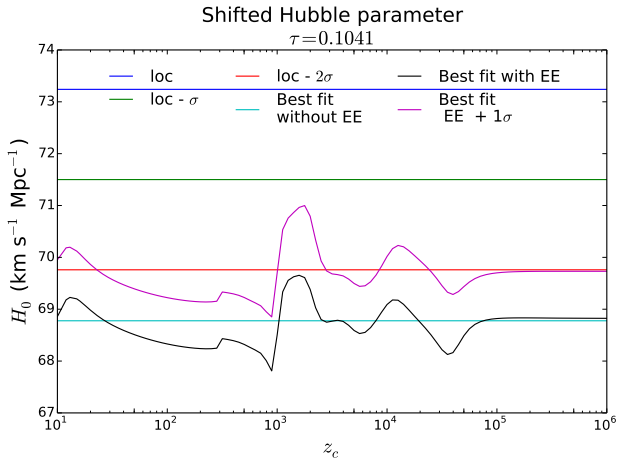

FIG. 10. The best-fit vales of H_0 (in km s^{-1} Mpc^{-1}) are shown with their 1σ errors. The local measurement is also shown at various σ.

The constraints we obtain on $\Omega_{\rm ee}$ are shown in Fig. 9. The change in the Hubble parameter is shown in Fig. 10.

Although fixing τ at 5σ does not entirely eliminate the discrepancy, H_0 is increased by a greater amount as compared to Fig. 8. For some z_c, it is increased to within the $2\sigma_{\rm loc}$ range of the locally measured Hubble parameter $H_{0,{\rm loc}}$. The greatest increase in the best-fit value of H_0 is 0.88 km s^{-1} Mpc^{-1} ($z_c = 1585$), in its 1σ value is 2.22 km s^{-1} Mpc^{-1} ($z_c = 1779$).

We plot 1σ likelihood ellipses for H_0 and $\Omega_{\rm ee}$ in Fig. 11. For local extrema in the shifts in H_0, a higher correlation between H_0 and $\Omega_{\rm ee}$ can be seen in the ellipses. While for critical redshifts that leave H_0 unchanged, there is little correlation between H_0 and $\Omega_{\rm ee}$. The Planck-16 values are always within $\sim 2\sigma$ ellipses and all the $\Omega_{\rm ee}$ estimators are consistent with the null result.

V. CONCLUSIONS

We consider a simple exotic energy density that provides a small perturbation to standard ΛCDM. The EE behaves like a cosmological constant until some critical redshift z_c, then decays away as a^{-6}. We investigate whether such an EE can alleviate the Hubble tension and find constraints on the maximum fractional energy density $\Omega_{\rm ee}$ today, that this field can have by doing a Fisher analysis on the Planck TT power spectrum.

In our analysis, we find that the value of τ places a strong constraint on the preferred value of $\Omega_{\rm ee}$ as well as the extent to which it can mitigate the Hubble tension. A larger value of τ leads, with EE, to a larger best-fit value of H_0.

In order for the best-fit value of H_0 for a ΛCMD + EE universe to coincide with the local measurement, a value of τ greater than its 5σ Planck-16 value is required. (Such a large value of τ is consistent with that obtained by the WMAP 9-year results, $\tau_{\rm WMAP} = 0.088 \pm 0.014$ [24].) If we fix τ at its Planck-16 best-fit and 2σ values, the tension is not altogether resolved, however, H_0 is shifted up closer to its local value. This is largely due to the error on H_0 increasing on the addition of the EE. Increasing τ and allowing for such an EE is indeed capable of alleviating the Hubble tension.

The Hubble tension between local measurements and the Planck data has been studied before by Ref. [3, 14, 25–31]. Altering the effective number of neutrino species $N_{\rm eff}$ [3] and allowing the equation of state parameter of dark energy w to vary with time [31] have been investigated as solutions to the Hubble tension (although variable w may introduce more tensions, eg. with BAO [31]). The correlation between H_0 and $N_{\rm eff}$ as well as that between H_0 and variable w is stronger than that between H_0 and the EE and they may be better candidates for diminishing the Hubble tension.

Furthermore, Ref. [3, 26, 32] suggest unresolved systematics in Planck data may be the cause of the tension. In particular, Ref. [32] suggests that Planck multipoles $\ell \geq 1000$ may suffer systematic errors. Excluding $\ell \geq 1000$ data not only significantly reduces the Hubble tension, but would also allow more room for early dark energy. However, Ref. [33] finds inconsistencies between high and low multipoles in Planck data statistically insignificant.

Adding the EE to ΛCDM, the cosmological parameters shift to accommodate the EE. The reduced χ^2 for the TT spectrum at their new best fit is not significantly changed. All changes in $\chi^2_{\rm red}$ are approximately an order smaller than the error on it. In Fig. 12, we plot the best-fit spectra without any EE and that with the EE which increases the best-fit vale of H_0 the most, for $\tau = 0.0774$. From the residues in the lower panel shown therein, it can be seen that the addition of the EE leaves the TT spectrum, and hence the reduced χ^2s, largely unaltered. Therefore, current data does not favor with statistical significance the addition of the EE to ΛCDM.

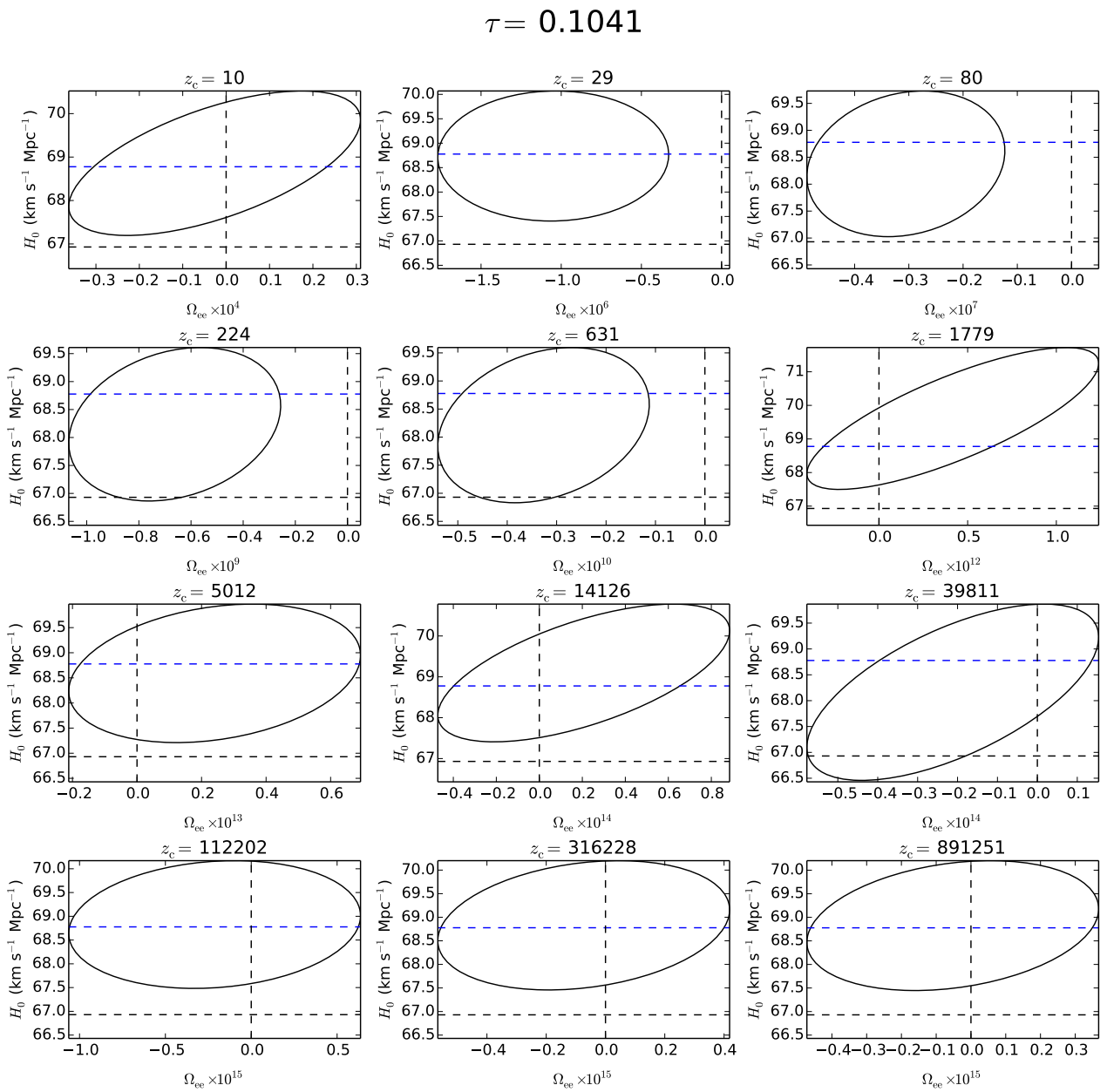

FIG. 11. We plot the 1σ likelihood contours for the Hubble parameter against $\Omega_{\rm ee}$ for various critical redshifts, covering the range of critical redshifts that we probe. We fix $\tau = \tau_{\rm Pl} + 5\sigma_{\tau,{\rm Pl}}$ for these. In each plot, the Planck-16 values for both parameters are marked by the horizontal and vertical dashed black lines. The dashed blue lines mark the value for the best-fit Hubble parameter for just the TT spectrum without EEs. Negative values of $\Omega_{\rm ee}$ are unphysical but allowed in our analysis. Estimators of $\Omega_{\rm ee}$ are consistent with zero within $\sim 2\sigma$.

This EE was motivated from axion-like fields that may explain dark energy [10]. The exotic energy considered here contributes its most to the total energy density of the Universe close to its critical redshift, forming its greatest fraction of the total energy density of the Universe. In Fig. 13 we plot this fraction $\eta = \rho_{\rm ee}(z_c)/\rho_{\Lambda{\rm CDM}}(z_c)$ of the total energy density of a pure ΛCDM universe that early exotic dark energy can from, as a function of redshift, according to our constraints on $\Omega_{\rm ee}$. For extremely high redshifts, the TT spectrum allows dark energy to have a larger energy density than that in a ΛCDM universe as long as it quickly redshifts away. This can also be seen from Fig. 1, where the EE with the greatest critical redshift has a higher energy density than radiation just before it decays. Closer to recombination, the greatest contribution of early dark

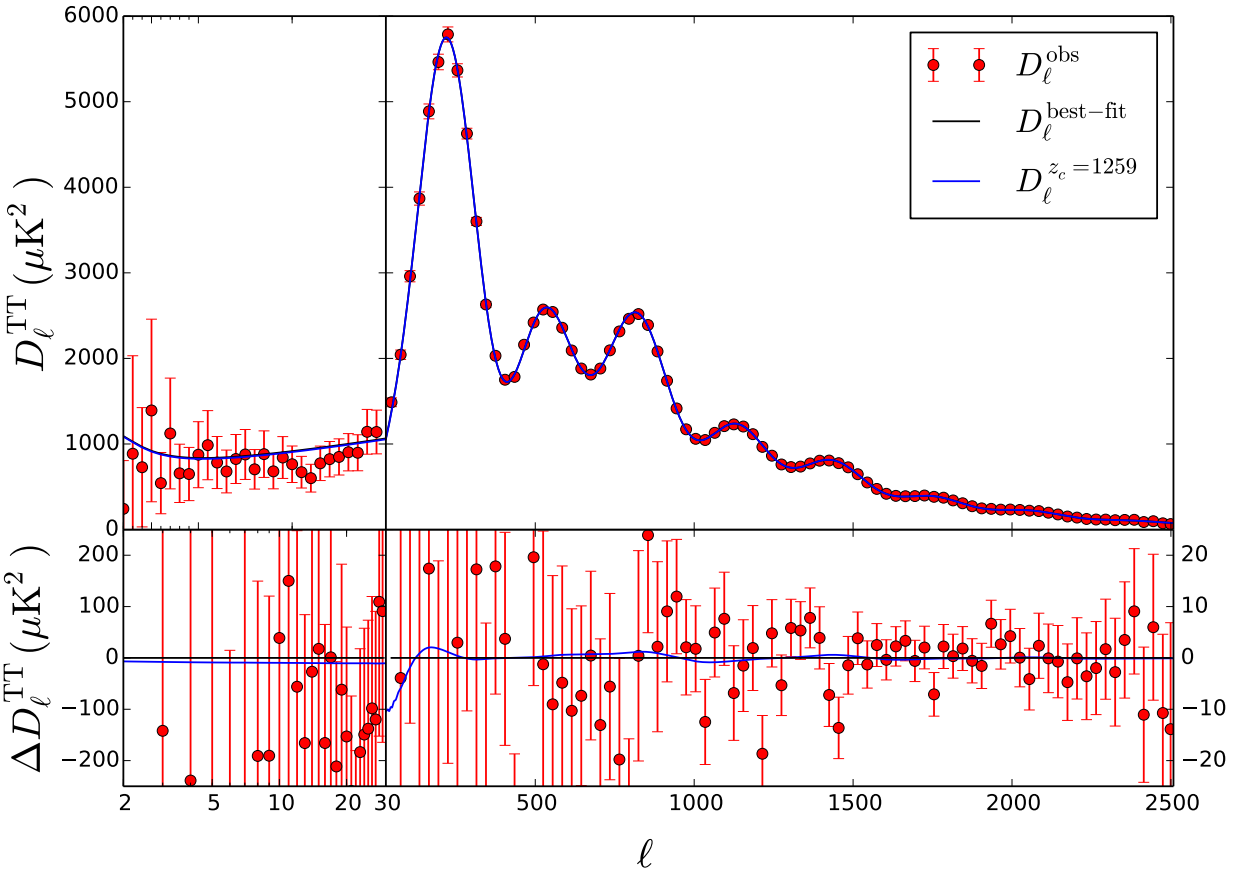

FIG. 12. We plot two best fits (blue and black) for the Planck temperature angular power spectrum for $\tau = \tau_{\rm Pl} + 2\sigma_{\tau,{\rm Pl}}$, and the Planck data (red). In black is the best fit without any EE. In blue we plot the best fit including an EE with $z_c = 1259$. This is the EE that increases the best-fit Hubble parameter the most. In the lower panel, we subtract $D_\ell^{\rm best-fit}$ from all three spectra and plot the residues. The bottom left and bottom right panels are scaled differently such that the residues may be more easily distinguishable.

energy is constraint to be $\lesssim 2\%$ of the total energy density in a ΛCDM universe. This result is consistent with constraints on other early dark energy models obtained through Monte Carlo analyses [11–13] that found upper limits of 4-5%.

The constraints presented here on $\Omega_{\rm ee}$ can be improved by more computationally heavy approaches such as including polarization data in the analysis or by doing a full MCMC on the 6 dimensional parameter space for each z_c considered. However, our simpler approach allows us to constrain an early dark energy model on a level consistent with a full MCMC analysis, and show that it is capable of increasing the value of the Hubble parameter. We conclude that adding an exotic energy, such as the one considered here, to ΛCDM may form a part of the solution to the Hubble tension if a higher optical depth to reionization is allowed. If the Hubble tension persists with a 1% measurement of the local value of H_0, then it may be useful to revisit the exotic-energy model considered here.

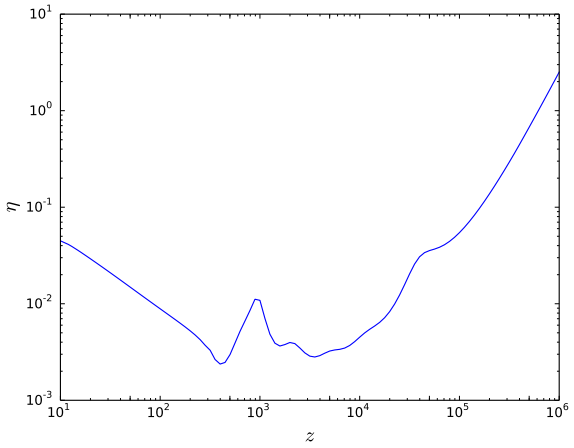

FIG. 13. The exotic energy density at its critical redshift $\rho_{\rm ee}(z_c)$ is plot as a fraction of the total energy density $\rho_{\Lambda{\rm CMD}}(z_c)$ of a pure ΛCDM universe for a range of redshifts. This fraction is within an order-unity factor of the greatest contribution of the EE to the energy density of the Universe. This plot was made for $\tau = \tau_{\rm Pl}$ and allowing $\Omega_{\rm ee} = \sigma_{\Omega_{\rm ee}}$.

VI. ACKNOWLEDGMENTS

We thank Julian Muñoz and Daniel Pfeffer for helpful discussions, and Adam Riess for useful comments on an earlier draft. This work was supported by NSF Grant No. 0244990, NASA NNX15AB18G, the John Templeton Foundation, and the Simons Foundation.

[1] P. A. R. Ade *et al.* (Planck), Astron. Astrophys. **571**, A16 (2014), arXiv:1303.5076 [astro-ph.CO].
[2] N. Aghanim *et al.* (Planck), (2016), arXiv:1605.02985 [astro-ph.CO].
[3] A. G. Riess *et al.*, Astrophys. J. **826**, 56 (2016), arXiv:1604.01424 [astro-ph.CO].
[4] V. Bonvin *et al.*, (2016), arXiv:1607.01790 [astro-ph.CO].
[5] R. R. Caldwell and M. Kamionkowski, Ann. Rev. Nucl. Part. Sci. **59**, 397 (2009), arXiv:0903.0866 [astro-ph.CO].
[6] P. Svrcek and E. Witten, JHEP **06**, 051 (2006), arXiv:hep-th/0605206 [hep-th].
[7] P. Svrcek, Submitted to: JHEP (2006), arXiv:hep-th/0607086 [hep-th].
[8] A. Arvanitaki, S. Dimopoulos, S. Dubovsky, N. Kaloper, and J. March-Russell, Phys. Rev. **D81**, 123530 (2010), arXiv:0905.4720 [hep-th].
[9] D. J. E. Marsh, Phys. Rev. **D83**, 123526 (2011), arXiv:1102.4851 [astro-ph.CO].
[10] M. Kamionkowski, J. Pradler, and D. G. E. Walker, Phys. Rev. Lett. **113**, 251302 (2014), arXiv:1409.0549 [hep-ph].
[11] M. Doran and G. Robbers, JCAP **0606**, 026 (2006), arXiv:astro-ph/0601544 [astro-ph].
[12] V. Pettorino, L. Amendola, and C. Wetterich, Phys. Rev. **D87**, 083009 (2013), arXiv:1301.5279 [astro-ph.CO].
[13] E. Calabrese, D. Huterer, E. V. Linder, A. Melchiorri, and L. Pagano, Phys. Rev. **D83**, 123504 (2011), arXiv:1103.4132 [astro-ph.CO].
[14] J. L. Bernal, L. Verde, and A. G. Riess, JCAP **1610**, 019 (2016), arXiv:1607.05617 [astro-ph.CO].
[15] D. Blas, J. Lesgourgues, and T. Tram, JCAP **1107**, 034 (2011), arXiv:1104.2933 [astro-ph.CO].
[16] R. R. Caldwell, R. Dave, and P. J. Steinhardt, Phys. Rev. Lett. **80**, 1582 (1998), arXiv:astro-ph/9708069 [astro-ph].
[17] G. Jungman, M. Kamionkowski, A. Kosowsky, and D. N. Spergel, Phys. Rev. **D54**, 1332 (1996), arXiv:astro-ph/9512139 [astro-ph].
[18] M. Tegmark, A. Taylor, and A. Heavens, Astrophys. J. **480**, 22 (1997), arXiv:astro-ph/9603021 [astro-ph].
[19] S. Galli, K. Benabed, F. Bouchet, J.-F. Cardoso, F. Elsner, E. Hivon, A. Mangilli, S. Prunet, and B. Wandelt, Phys. Rev. **D90**, 063504 (2014), arXiv:1403.5271 [astro-ph.CO].
[20] J. B. Muñoz, D. Grin, L. Dai, M. Kamionkowski, and E. D. Kovetz, Phys. Rev. **D93**, 043008 (2016), arXiv:1511.04441 [astro-ph.CO].
[21] M. Zaldarriaga, Phys. Rev. **D55**, 1822 (1997), arXiv:astro-ph/9608050 [astro-ph].
[22] D. Coe, (2009), arXiv:0906.4123 [astro-ph.IM].
[23] P. A. R. Ade *et al.* (Planck), Astron. Astrophys. **571**, A15 (2014), arXiv:1303.5075 [astro-ph.CO].
[24] G. Hinshaw *et al.* (WMAP), Astrophys. J. Suppl. **208**, 19 (2013), arXiv:1212.5226 [astro-ph.CO].
[25] E. Di Valentino, A. Melchiorri, and J. Silk, Phys. Lett. **B761**, 242 (2016), arXiv:1606.00634 [astro-ph.CO].
[26] S. Grandis, D. Rapetti, A. Saro, J. J. Mohr, and J. P. Dietrich, (2016), 10.1093/mnras/stw2028, arXiv:1604.06463 [astro-ph.CO].
[27] M. Archidiacono, S. Gariazzo, C. Giunti, S. Hannestad, R. Hansen, M. Laveder, and T. Tram, JCAP **1608**, 067 (2016), arXiv:1606.07673 [astro-ph.CO].
[28] C. Umilt, M. Ballardini, F. Finelli, and D. Paoletti, JCAP **1508**, 017 (2015), arXiv:1507.00718 [astro-ph.CO].
[29] Z. Huang, Phys. Rev. **D93**, 043538 (2016), arXiv:1511.02808 [astro-ph.CO].
[30] P. A. R. Ade *et al.* (Planck), Astron. Astrophys. **594**, A14 (2016), arXiv:1502.01590 [astro-ph.CO].
[31] S. Joudaki *et al.*, (2016), arXiv:1610.04606 [astro-ph.CO].
[32] G. E. Addison, Y. Huang, D. J. Watts, C. L. Bennett, M. Halpern, G. Hinshaw, and J. L. Weiland, Astrophys. J. **818**, 132 (2016), arXiv:1511.00055 [astro-ph.CO].
[33] N. Aghanim *et al.* (Planck), (2016), arXiv:1608.02487 [astro-ph.CO].